THE JOURNAL OF PHYSICAL CHEMISTRY B

ARTICLE

pubs.acs.org/JPCB

Solubility of Aliphatic Hydrocarbons in Piperidinium Ionic Liquids: Measurements and Modeling in Terms of Perturbed-Chain Statistical Associating Fluid Theory and Nonrandom Hydrogen-Bonding Theory

Kamil Paduszyński* and Urszula Domańska

Department of Physical Chemistry, Faculty of Chemistry, Warsaw University of Technology, Noakowskiego 3, 00-664 Warsaw, Poland

ABSTRACT: Ionic liquids (ILs) reveal many unique properties which make them very interesting for applications in modern "green" technologies. For that reason, detailed knowledge about correlations between the ions' structure, their combinations, and the bulk properties is of great importance. That knowledge can be accessed by reliable measurements and modeling of systems with ILs in terms of various theoretical approaches. In this paper we report new experimental results on liquid−liquid equilibrium (LLE) measurements of 10 binary systems composed of piperidinium ILs [namely, 1-propyl-1-methylpiperidinium bis(trifluoromethylsulfonyl)imide and 1-butyl-1-methylpiperidinium bis(trifluoromethylsulfonyl)imide] and aliphatic hydrocarbons (*n*-hexane, *n*-heptane, *n*-octane, cyclohexane, and cycloheptane). Moreover, new results on liquid density of pure 1-butyl-1-methylpiperidinium bis(trifluoromethylsulfonyl)imide are presented. Upper critical solution temperature type of phase behavior for all studied systems was observed. Decrease of solubility of *n*-alkane with an increase of its alkyl chain length and increase of solubility when changing linear into cyclic structure of hydrocarbon were detected. LLE modeling of investigated systems was performed in terms of two modern theories, namely, perturbed-chain statistical associating fluid theory (PC-SAFT) and nonrandom hydrogen-bonding theory (NRHB). Pure fluid parameters of the models were obtained from fitting of experimental liquid density and solubility parameter data at ambient pressure and tested against high pressure densities. Then literature values of activity coefficients of *n*-alkanes and cycloalkanes at infinitely diluted mixtures with ILs were used to optimize binary interaction parameters of the models. Finally, the LLE phase diagrams were calculated with average absolute relative deviations of 4.1% and 3.4% of the IL mole fraction for PC-SAFT and NRHB, respectively. The PC-SAFT and NRHB models were both able to capture phase behavior in a qualitative manner. Both models predict the order in which solubility of hydrocarbon in the IL increases, including the effects of chain length of *n*-alkane as well as chain length of alkyl substituent in piperidinium cation. Moreover, predicted solubility of cycloalkanes is also higher than that of respective *n*-alkanes. Our results suggest that the presented approach of PC-SAFT and NRHB modeling can be successfully applied to cross-associating systems as well. In summary, we have shown that relatively good results can be obtained for such complex systems by using quite simple molecular models and combining rules. To the best of our knowledge, this is the very first paper in which such equation-of-state modeling has been adopted for systems with ILs.

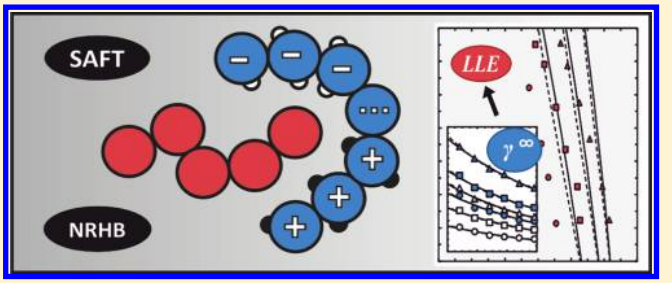

INTRODUCTION

Ionic liquids (ILs) are a broad family of molten salts composed of organic or inorganic ions differing significantly in size and shape. Asymmetry between cation and anion allows them to exist in liquid phase at room temperature as well as to reveal many interesting properties such as extremely low vapor pressures and high stability. The diversity of cation−anion combinations enables the design of task-specific ILs. Because of all these properties, ILs have seemed to be very attractive for many areas of pure and applied sciences for the last two decades. Nowadays, they are viewed as a new class of environmentally friendly solvents for various applications in chemical engineering,[1] biotechnology,[2] pharmaceutical systems,[3] supercritical fluids processes,[4] biocatalysis,[5] electrochemistry,[6] and solar energy storage.[7] In particular, many potential applications of ILs in the chemical industry, specifically in separations processes, have been proposed and investigated experimentally as well as theoretically. For example, due to high selectivity in the separation of thiophene and other sulfur compounds from alkanes, they are seriously considered as a new class of solvents for liquid−liquid extraction units of new technologies for gasoline and diesel desulfurization.[8−10] The concept of separation of gaseous mixtures as well as absorption of current postcombustion CO_2 by use of ILs has been proposed as well and is still extensively and widely studied.[11−13]

Therefore, systematic investigations on physical and thermodynamic properties for systems containing ILs are of great importance. The major part of experimental research we conduct in our laboratory is focused on determination and modeling of physical and thermodynamic properties of pure ILs and their mixtures with common organic solvents and water. We determine

Received: May 30, 2011
Revised: September 21, 2011
Published: September 26, 2011

dx.doi.org/10.1021/jp205048b | *J. Phys. Chem. B* 2011, 115, 12537–12548

solid−liquid, liquid−liquid, and vapor−liquid equilibria (SLE, LLE, and VLE) for binary or ternary systems with IL as well as limiting activity coefficients of various solutes in ILs. We determine volumetric, transport, and interfacial properties of such systems as a function of temperature and pressure as well. Recently ILs based on 1-alkyl-1-methylpiperidinium cation have received much of our attention.[14−18] We reported SLE and LLE in binary systems of ILs 1-ethyl-1-methylpiperidinium bis(trifluoromethylsulfonyl)-imide,[16] 1-methyl-1-propylpiperidinium bis(trifluoromethylsulfonyl)imide,[17] and 1-butyl-1-methylpiperidinium thiocyanate[16] (abbreviated [EMPIP][NTf_2], [PMPIP][NTf_2], and [BMPIP]-[SCN], respectively) with water, or alcohol, or aliphatic hydrocarbons. Moreover, we measured limiting activity coefficients of various organic solutes and water in [PMPIP][NTf_2],[14] [BMPIP][NTf_2],[18] and [BMPIP][SCN].[15] In literature, piperidinium ILs are described mainly in the context of their physical and electrochemical properties.[19−26] However, mutual solubilities of [PMPIP][NTf_2] and water[27,28] as well as densities of this IL at elevated temperature and pressure[29] were also reported.

There is no doubt that, apart from experimental efforts, the modeling of systems containing ILs is also of great importance. Modeling allows us to understand origins of measured properties and then to predict and control them to obtain products appropriate for specific applications. However, the lack of experimental data, mainly pure IL vapor pressures, makes determination of model-specific parameters impossible and thus obstructs the ability to predict properties for multicomponent systems. The molecular complexity of IL-based systems, in turn, causes ambiguity when one chooses a molecular picture describing IL structure and interactions. Therefore, modeling of systems with ILs is challenging task. For a comprehensive review of the state of the art on the topic, the reader is referred to Vega et al.[30]

In spite of the mentioned difficulties and problems, many attempts have been made to reproduce thermodynamic properties by use of various models differing in complexity and physical foundations. It was shown by a few authors that simple expressions for excess Gibbs energy, such as nonrandom two-liquid model (NRTL) and universal quasi-chemical activity coefficient (UNIQUAC), as well as cubic equations of state can be successfully applied for binary SLE, LLE, and VLE correlations.[16,31,32] Group-contribution idea-based modified universal functional activity coefficient (UNIFAC) (Dortmund) has predictive ability, but the parameter matrix is still limited to merely a few ions.[33] The main disadvantage of this model is that determination of parameters for new functional groups requires a large amount of experimental information about binary systems. In spite of that, the model is able to describe VLE, excess enthalpies, and activity coefficients at infinite dilution data simultaneously.[33]

Recently, statistical associating fluid theory (SAFT)[34,35] and its various modifications (PC-SAFT,[36,37] soft-SAFT,[38] tPC-SAFT[39,40]) as well as lattice theory-based models (for example, nonrandom hydrogen-bonding model, NRHB,[41,42] or the model developed by Xu et al.[43]) have become very popular. However, systems containing only 1-alkyl-3-methylimidazolium ionic liquids (ImILs) have been considered so far. Since this paper is concerned with application of particular members of this family of models, we present a short review of current status in this field.

Perturbed-chain statistical associating fluid theory[36,37] (PC-SAFT) has been very recently applied to model density over a wide pressure range, and VLE phase behavior has been observed for a binary system of 1-butyl-3-methylimidazolium tetrafluoroborate with 2,2,2-trifluoroethanol.[44] The authors obtained pure fluid model parameters from atmospheric pressure density. Then they predicted high pressure densities of the IL. The results were not in good agreement with reported experimental data. Finally, they performed calculations of VLE in binary systems under study, obtaining good results only when binary interaction correction was adopted.

In turn, Andreu and Vega[45] applied the soft-SAFT[38] model to reproduce solubility of CO_2 in ImILs with hexafluorophospate or tetrafluoroborate anion. They showed that soft-SAFT is capable of describing the physical absorption of different gases in those ILs with good accuracy. The authors modeled ILs as neutral ion pairs forming Lennard-Jones chains with one associating site in each molecule, mimicking the specific interactions between the cation and the anion as a pair because of the charges and the asymmetry. In further work, the same authors extended the model applications for ImILs with [NTf_2] anion.[46] They modeled solubility of CO_2, H_2, and Xe in those ILs by assuming three associating sites per IL ion pair: one A site and two B sites. An A site corresponds to the nitrogen atom in the imidazolium ring, and a B site represents the delocalized charge due to the oxygen molecules on the anion. On the basis of obtained results, they concluded that soft-SAFT is able to describe the physical absorption of different gases in ILs with good accuracy, in spite of the most complex nature of the system.[45,46]

Another very interesting contribution presenting soft-SAFT modeling of [NTf_2]-based ImILs was published very recently by Llovell et al.[47] The authors updated the model's parameters of Andreu and Vega[45] by using newly available experimental data on liquid density. Then they tested the parameters by calculation of literature properties of pure ILs and their mixtures (high pressure densities and isothermal compressibility calculated from parameters fitted to atmospheric pressure data, surface tension calculated from density gradient theory, and densities of IL binary mixtures) and phase diagrams of binary systems (VLE and LLE for systems of IL with water or alcohol) in a totally predictive manner. Obtained results were found to be in excellent agreement with experimental data. Only in the case of LLE did the predictions without binary corrections of Lorentz−Berthelot mixing rules not result in quantitative agreement.

Another SAFT approach reported as a tool for IL system modeling is truncated perturbed-chain polar statistical associating fluid theory (tPC-PSAFT).[39,40] Again, CO_2 solubility in ImILs has been studied. In the work presented by Kroon et al.,[48] parameters for tetrafluoroborate- and hexafluorophosphate-based ImILs were estimated on the basis of IL experimental thermodynamic and physicochemical data separately for each ion. Then parameters for the total pure ILs were calculated via standard combining rules. In the successive work,[49] the same authors recalculated those parameters by using standard procedure, namely, fitting them to experimental liquid density data and estimated values of vapor pressures. Both authors did not consider association contribution in the case of pure ILs, while they took into account dipolar interactions of IL molecules and quadrupolar interactions of CO_2 molecules. In the case of ILs, they assumed that their polarity is comparable to the polarity of lower to medium alcohols. Therefore, the permanent dipole moment of 1.70 D has been assigned to each IL molecule. The cross-association IL−CO_2 was taken into account, and the described model's parameters were obtained from thermodynamic functions of dissolution of CO_2 in IL.

Among lattice theory-based equations of state, the nonrandom hydrogen-bonding (NRHB) model[41,42] seems to be

very promising for modeling of systems with ILs. Recently, Tsioptsias et al.[50] reported NRHB calculations of systems with $[NTf_2]$-based ImILs. Pure ILs were modeled as composed of strongly associating neutral ion pairs. The strength of association was assumed to be related to the number of associating sites per ion pair, while the number of associating sites can be chosen arbitrarily and reflects the assumption that ion−ion electrostatic interactions are accounted for as strong specific interactions. The authors assumed that there are five negative (acceptor) and five positive (donor) sites. Then pure IL parameters were determined by fitting of experimental liquid density data over a wide range of pressure and IL solubility parameters. On the basis of performed parametrization of pure components, binary LLE and VLE for the systems ImIL + alcohol, ImIL + water, or ImIL + CO_2 were calculated. Calculations revealed that, to obtain good agreement with experimental results, two additional adjustable parameters are required. One of them corresponds to cross-association, while the second is a binary correction to conventional mixing rules for cross-dispersive energy. The same approach was adopted recently by Paduszyński et al.[17] to model binary LLE for binary systems containing $[PMPIP][NTf_2]$ and linear alcohol (from 1-pentanol to 1-undecanol). In this case NRHB theory (as well as PC-SAFT) was not able to predict liquid−liquid splitting in those systems. Therefore, a temperature-dependent binary interaction parameter was introduced to correlate experimental data with good accuracy. Parameters related to cross-association, however, were calculated by using standard mixing rules.

This paper is a continuation of our systematic study on piperidinium ILs. We report new experimental density data for pure $[BMPIP][NTf_2]$ at ambient pressure and new LLE data for binary systems containing $[PMPIP][NTf_2]$ or $[BMPIP][NTf_2]$ and *n*-alkane (*n*-hexane, *n*-heptane, or *n*-octane) or cycloalkane (cyclohexane or cycloheptane). Then we present modeling of studied systems in terms of PC-SAFT and NRHB models. Pure fluid parameters for $[BMPIP][NTf_2]$ have been determined from measured IL density and literature total solubility parameters.[51] Then limiting activity coefficients of hydrocarbons in ILs and LLE phase diagrams have been calculated on the basis of a procedure proposed by Schacht et al.[52] According to this method, binary interaction corrections were obtained by adjusting them to literature values of limiting activity coefficients of respective hydrocarbons in $[PMPIP][NTf_2]$[14] or $[BMPIP][NTf_2]$.[18] Then the resulting values were used to calculate LLE. To the best of our knowledge, this is the very first paper in which such a method of modeling has been adopted for IL systems. Moreover, we confirmed that presented approach is applicable to cross-associating systems such as IL + alcohol or IL + water.

EXPERIMENTAL PROCEDURES

Materials. The ionic liquids 1-methyl-1propylpiperidinium bis(trifluoromethylsulfonyl)imide $[PMPIP][NTf_2]$ and 1-butyl-1-methylpiperidinium bis(trifluoromethylsulfonyl)imide $[BMPIP][NTf_2]$ had a mass fraction purity of >0.99 and were purchased from IoLiTec (Ionic Liquids Technologies GmbH, Germany). The structure of the investigated ILs is presented in Figure 1. The ILs were further purified by subjecting the liquid to a low pressure of about 1 mPa at a temperature about 368 K for ca. 48 h. This procedure removed any volatile chemicals and water from the ionic liquid. The list of hydrocarbons used in this study, including source and grade, is as follows: *n*-hexane, Fluka, >0.997; *n*-heptane, Sigma−Aldrich; *n*-octane, Sigma−Aldrich, >0.995; cyclohexane, Sigma−Aldrich, >0.997; cycloheptane, Sigma−Aldrich, >0.98. All compounds were checked by gas−liquid chromatography analysis, and no significant impurities were found. Therefore they were used as obtained without further purification.

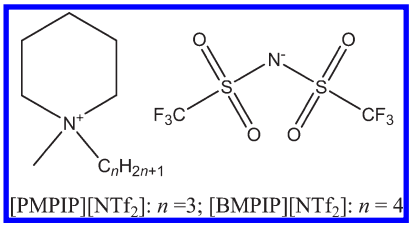

Figure 1. Chemical structures of investigated piperidinium ILs: 1-propyl-1-methylpiperidinium bis(trifluoromethylsulfonyl)imide ($[PMPIP][NTf_2]$) and 1-butyl-1-methylpiperidinium bis(trifluoromethylsulfonyl)imide ($[BMPIP][NTf_2]$).

Water Content. Water content was analyzed by the Karl Fischer titration technique (Schott Instruments Titro-Line KF). A sample of the IL was dissolved in methanol and titrated with steps of 2.5 μL. The results obtained have shown the water content to be less than 250 ppm. The titrant CombiTitrant 5 (no. 1.8805.1000, Merck; one-component reagent for volumetric Karl Fischer titration) was used. The lower determination limit of this technique is approximately 50−100 ppm H_2O.

Density Measurements. The density of the $[BMPIP][NTf_2]$ IL at atmospheric pressure was measured at temperature range T = 293.15−363.15 K by use of an Anton Paar GmbH 4500 vibrating tube densimeter (Graz, Austria), thermostated at different temperatures. Two integrated Pt 100 platinum thermometers provided good internal precision in temperature control (±0.01 K). The densimeter includes an automatic correction for the viscosity of the sample. The calibration for temperature and pressure was made by the instrument supplier. The apparatus is precise to within 10^{-5} g·cm^{-3}, and the uncertainty of the measurements was estimated to be better than 10^{-4} g·cm^{-3}. The densimeter's calibration was performed at atmospheric pressure with doubly distilled and degassed water, specially purified benzene (Chemipan, Poland, > 0.99 mol fraction), and dried air.

Liquid−Liquid Phase Equilibria Apparatus and Measurements. Two phases disappearance observed with an increasing temperature regime have been determined by a synthetic method.[53] Mixtures of the IL and hydrocarbon were prepared by weighing pure components to within 10^{-4} g. The sample of solute and solvent was heated very slowly (at heating rate less than 2 K·h^{-1} near the equilibrium temperature) with continuous stirring inside a Pyrex glass cell, placed in a thermostat. The dimensions of the cell are internal diameter 2 cm and height 2 cm. The foggy solution disappearance temperature detected visually was measured by calibrated electronic thermometer P 550 (Dostmann Electronic GmbH, Germany). For each system the reproducibility was tested once. The temperature of two phases' disappearance corresponding to liquid−liquid equilibrium was observed visually. The reproducibility of the LLE experimental points was ±0.1 K.

THEORETICAL BACKGROUND

Perturbed-Chain Statistical Associating Fluid Theory. Statistical associating fluid theory (SAFT) models real fluids' molecules as chains built of physically and specifically interacting

segments. Original SAFT was developed by Chapman et al.[34,35] and was based on Wertheim's first-order thermodynamic perturbation theory[54,55] in the beginning of 1990s. Since then many modifications and extensions of original SAFT equations have been proposed. The current status, advantages, and applications of various SAFT-related approaches have been extensively reviewed in the literature.[56−58]

One of the most popular and the most widely applied version of SAFT is perturbed-chain statistical associating fluid theory (PC-SAFT), proposed by Gross and Sadowski.[36,37] In comparison to its previous version, the hard-sphere reference fluid is replaced by a hard-chain fluid. Weak dispersion interactions, association, and other types of interactions are considered as a perturbation of the reference fluid. A detailed description and derivation of the PC-SAFT particular terms were described elsewhere.[36,37] In this paper we only introduce the model characteristic parameters.

In terms of SAFT the thermodynamics of a mixture is fully characterized by an expression giving the relation between its residual Helmholtz free energy (A^{res}) and state parameters, namely, temperature, number density, and composition, given at most by numbers of molecules or by mole fractions of all components. All the other useful expressions such as pressure or fugacity coefficient can be calculated as some derivative of A^{res} according to general thermodynamic relations. In the original PC-SAFT, the following effects were taken into consideration explicitly as individual contributions to A^{res}: chain reference fluid (hc), dispersive interactions (disp), dipole−dipole interactions (polar), and association (assoc):

$$\tilde{a}^{res} \equiv \frac{A^{res}}{Nk_BT} = \tilde{a}^{hc} + \tilde{a}^{disp} + \tilde{a}^{polar} + \tilde{a}^{assoc} \quad (1)$$

where N stands for number of molecules in the system and k_B is the Boltzmann constant. For systems that contain only nonassociating components, only the first two terms are included. Each nonpolar component is then characterized by three characteristic parameters: number of spherical segments forming the chain (m), temperature-independent hard-sphere segment diameter (σ), and depth of the dispersion energy potential (ε). In the case of polar components, dipole moment (μ) and at most one additional parameter related to dipolar interactions need to be specified. The number of additional parameters depends on the term $\tilde{a}^{polar}$ in eq 1. Three most popular terms are those reported by Gross and Vrabec,[59] Jog and Chapman,[60] and Karakatsani et al.[61] For systems that contain associating components (e.g., water, alcohols, amines, etc.), an association contribution in eq 1 becomes essential. Such a system is additionally characterized by the presence of different types of associating sites (denoted by A, B, ...) attached to molecules of different components. To characterize a particular AB interaction, two additional parameters (per pair of sites) describing the strength of association are introduced: energy potential well depth (ε^{AB}) and volume (κ^{AB}) of association AB. A common procedure for calculating all those parameters rests on adjusting them to pure substance properties such as saturated liquid or vapor densities or vapor pressures.

Nonrandom Hydrogen-Bonding Theory. Nonrandom hydrogen-bonding theory[41,42] (NRHB) belongs to the family of compressible lattice theory-based models. In terms of NRHB, molecules are viewed as composed of segments filling quasi-crystalline lattice. However, empty segments are allowed to be present in the lattice as well. They account for density dependence on temperature and pressure. Nonrandom distribution of molecular and holes is governed by Guggenheim quasi-chemical approximation, while association contribution is determined by Veytsman's statistics. As in the case of PC-SAFT, we present here only the model parameters. For detailed descriptions and derivations, the reader is referred to the original papers.[41,42]

Pure nonassociating fluid is characterized by three parameters: average interaction energy per segment (ε^*), close-packed specific volume (v_{sp}^*), and surface-to-volume ratio (s). The parameters ε^* and v_{sp}^* are assumed to be temperature-dependent:

$$\begin{aligned} \varepsilon^* &= \varepsilon_h^* + \varepsilon_s^*(T - 298.15\ \mathrm{K}) \\ v_{sp}^* &= v_{sp,0}^* + v_{sp,1}^*(T - 298.15\ \mathrm{K}) \end{aligned} \quad (2)$$

Subscripts h and s refer to enthalpic and entropic contributions to dispersive energy, respectively. The parameter $v_{sp,1}^*$ is treated as a characteristic parameter for different homologous series.[42] If the fluid's molecules are built of r segments and have zq external contacts (where z is the lattice coordination number), the parameter s is defined $s = q/r$. It can be treated as an adjustable parameter or calculated from UNIQUAC molecular volume and area parameters or from a group-contribution model such as UNIFAC. For associating fluids, donor and acceptor groups need to be distinguished and then additional parameters related to association are introduced. Per one donor group α and acceptor group β, three parameters are specified: energy ($E_{\alpha\beta}^H$), entropy ($S_{\alpha\beta}^H$), and volume change ($V_{\alpha\beta}^H$) due to formation of $\alpha-\beta$ complex. Volume change due to association is usually set equal to zero. It was shown that such an assumption does not affect the model's performance and reduces the number of adjustable parameters.

Molecular Models. To apply PC-SAFT or NRHB theories for accurate predictions of thermodynamic properties of pure fluid and mixtures, a physically meaningful molecular model is required. Such a model should be able to capture basic physical characteristics of the substance and should be based on parameters determined from reliable experimental data. In the case of ILs, however, the problem is not easy to overcome, as they are very complex systems exhibiting different kinds of interactions at molecular level. Dispersive and polar−electrostatic interactions[62] as well as ion pairing[63−66] have essential significance in those systems, as does nanostructural organization coming out of molecular dynamics simulations[67] and small-wide-angle X-ray scattering (SWAXS) experiments.[68] Therefore, some simplifying assumptions have to be made to model such fluids with the models presented above.

For the PC-SAFT and NRHB models, we follow the methodology originally proposed by Tsioptsias et al.[50] and recently applied by us to model [PMPIP][NTf_2] + alcohol binary systems.[17] According to this approach, physical (dispersive) and specific interactions are taken into account explicitly, while other types of interactions such as ionic, polar, and specific are not treated separately but are included in one kind of strong specific interactions. In our previous paper,[17] we modified this assumption in the case of PC-SAFT, where dipolar interactions were accounted for explicitly by a Gross−Vrabec term.[59] However, in this work we noticed that the influence of this term on pure properties of ILs is negligible. Thus, we did not include dipole−dipole interactions in the molecular models of ILs without recalculating the parameters.

Considering the ionic interactions as strong specific interactions can be justified due to theoretical as well as experimental and computational evidence. Different investigations showed that, in pure ILs, cations and anions are associated together, forming neutral ionic pairs or hydrogen-bonding ionic clusters in the bulk liquid state.[62−68] Besides, the bulky size and asymmetric charge distribution of molecular ions softens electrostatic forces and thus highly directional interactions of shorter range are generated. Asymmetric charge distributions give rise to dipolar and higher multipolar interaction to the charge−charge interactions. This fact justifies the use of specific associating sites in order to mimic the strong interactions between ions. Moreover, delocalization of the electric charge due to the oxygen groups in $[NTf_2]$ anion enhances the possibility of interaction with the surrounding cations through them, as well as with the associating sites of other components in a mixture.[45,46]

Therefore, the investigated ionic liquids $[PMPIP][NTf_2]$ and $[BMPIP][NTf_2]$ are modeled as a substance composed of strongly associating chain molecules. According to the proposed model, we used an A_1 site to represent a positive group corresponding to the positive charge of the cation and its proximity and a B_1 site to represent a negative site corresponding to the delocalized charge on the anion. Each type of associating site is identically defined, but only A_1B_1 interactions between different IL molecules are allowed. The strength of association is reflected by the parameters of the respective model and the number of associating sites per molecule.

In the case of pure hydrocarbons, the molecular model is much easier to define, as their chemical structure and interactions are well suited to both molecular pictures presented in the PC-SAFT and NRHB approaches. They are modeled as chain molecules built of segments interacting by dispersive forces. Association occurs only in pure ILs.

Binary Interaction Parameter. To apply PC-SAFT or NRHB models to mixtures, one need to assume combining rules for cross-interaction parameters. It was found that good model performance is obtained when standard quadratic mixing rules of Lorentz−Berthelot are adopted. In the case of PC-SAFT we used[36]

$$\varepsilon_{ij} = \sqrt{\varepsilon_i \varepsilon_j}(1 - k_{ij}) \qquad \sigma_{ij} = \frac{\sigma_i + \sigma_j}{2} \tag{3}$$

whereas for NRHB we used[42]

$$\varepsilon^*_{ij} = \sqrt{\varepsilon^*_i \varepsilon^*_j}(1 - k_{ij}) \tag{4}$$

where k_{ij} is the binary interaction parameter for pair ij of components ($k_{ij} = k_{ji}$). If k_{ij} values are set equal to zero, the models are used in a totally predictive manner. However only in the case of simple systems containing sufficiently similar substances can good predictive quality be exhibited. Therefore, the parameters

Table 1. Summary of Experimental and Literature Liquid Density Data for $[BMPIP][NTf_2]$ IL as a Function of Temperature

	ρ (g·cm^{-3})	
T (K)	this work	literature
293.15	1.3835	1.384[a]
298.15	1.3791	1.379 98;[b] 1.3786[c]
303.15	1.3748	1.373 74[b]
308.15	1.3706	1.369 04[b]
313.15	1.3663	1.364 57[b]
318.15	1.3621	1.360 56[b]
323.15	1.3579	1.356 90[b]
328.15	1.3536	1.353 47[b]
333.15	1.3494	1.350 48[b]
338.15	1.3452	1.347 72[b]
343.15	1.3410	1.345 28[b]
348.15	1.3369	
353.15	1.3327	
358.15	1.3285	
363.15	1.3243	

[a] Reference 26. [b] Reference 19. [c] Reference 69.

Table 2. Experimental Binary LLE Data for Investigated Binary Systems (IL + Hydrocarbon)

n-hexane		*n*-heptane		*n*-octane		cyclohexane		cycloheptane	
x_1	T (K)	x_1	T (K)	x_1	T (K)	x_1	T (K)	x_1	T (K)
					$[PMPIP][NTf_2]$				
0.9399	301.4	0.9361	326.3	0.9655	296.8	0.8156	346.4	0.9082	309.1
0.9370	305.7	0.9129	352.6	0.9554	322.6	0.7908	353.8	0.8945	321.5
0.9292	310.4	0.9059	357.4	0.9430	343.7	0.8873	307.6	0.8690	335.2
0.9188	319	0.9447	313.7	0.9355	358.4	0.8597	325.4	0.8150	363.7
0.9072	326.4	0.9278	334.9	0.9629	307.7	0.8453	333.2	0.8622	341.4
0.9135	323	0.9200	345.3	0.9497	333.3	0.8756	315.8	0.8408	351.9
		0.9515	305.6	0.9395	351.7	0.8293	340.8		
					$[BMPIP][NTf_2]$				
0.8655	325.2	0.9093	322.4	0.9575	312.4	0.7908	311.5	0.8501	303.8
0.8364	352.1	0.9137	312.3	0.9279	336.7	0.7512	336.9	0.8214	328.3
0.8772	311.4	0.8595	359.1	0.9123	347.6	0.7356	345.1	0.7434	364.1
0.8550	335.3	0.8458	365.1	0.8840	365.5	0.7704	322.1	0.8450	311.7
		0.8774	346.2	0.9470	322.4	0.7608	329.6	0.7929	343.7
		0.8912	333.6	0.8944	358.7			0.7686	354.6

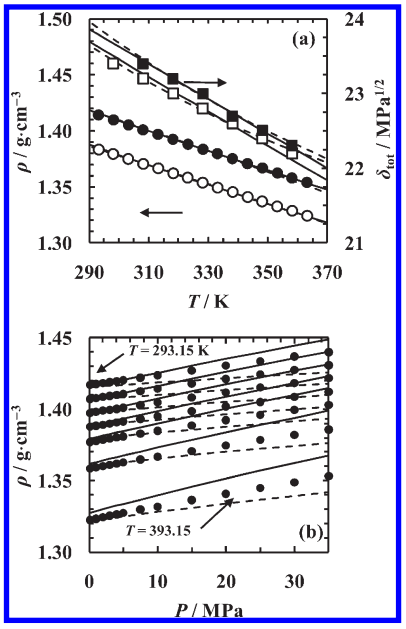

Figure 2. Experimental and calculated properties of pure ILs. (a) Liquid density (●, [PMPIP][NTf_2];[17] ○, [BMPIP][NTf_2]) and total solubility parameters δ_{tot} (■, [PMPIP][NTf_2];[51] □, [BMPIP][NTf_2][51]). (b) High-pressure densities of [PMPIP][NTf_2][29] at T = 293.15, 303.15, 313.15, 323.15, 333.15, 353.15, and 393.15 K. (—) PC-SAFT model; (---) NRHB model. See text for details.

are usually adjusted to experimental binary data to obtain good agreement between measured and calculated results. It would be interesting to calculate the binary interaction parameters from one type of binary data and then to use the obtained values in calculations of other types of binary data. For example, one could correlate binary VLE data and then use calculated parameters k_{ij} to predict excess enthalpies of mixing. Another methodology was proposed recently by Schacht et al.[52] To predict binary VLE phase diagrams, the authors used PC-SAFT binary interaction parameters determined from experimental infinite dilution activity coefficients or Henry's constants of one of the components from the system in another. To calculate the activity coefficient of component i (solute) in infinitely diluted mixture with component j (solvent), one need to use a known thermodynamic expression:

$$\gamma_i^{\infty} = \frac{\phi_i^{L,\infty}}{\phi_i^{L,0}} \tag{5}$$

where $\varphi_i^{L,\infty}$ and $\varphi_i^{L,0}$ denote fugacity coefficients of the solute at infinitely diluted mixture with solvent and pure (real or hypothetical) state, respectively. The expressions for φ_i^{L} as a function of temperature, pressure, and composition can be derived from PC-SAFT and NRHB equations of state. Results presented in this paper confirmed that reliable data of limiting activity coefficients are meaningful for estimating the full phase behavior of mixtures. The major advantage of this method is that the numerous values of limiting activity coefficients for various systems are available in comprehensive databases. On the other hand, they can be easily measured by gas−liquid chromatography (GLC)[14,15,18] or accurately predicted by group-contribution models, for example, modified UNIFAC (Dortmund).[33] Then the described approach could be fully predictive, since only pure substance parameters for equation of state and chemical structures for

Table 3. PC-SAFT Pure Fluid Molecular Parameters for ILs and Other Substances Investigated in This Work[a]

				% AARD[b]		
fluid	m	σ (Å)	ε/k_B (K)	ρ	P	δ_{tot}
[PMPIP][NTf_2][c]	8.8514	3.7083	226.58	<0.1		0.1
[BMPIP][NTf_2][d]	9.1307	3.7414	233.19	<0.1		0.2
n-hexane[e]	3.0576	3.7983	236.77	0.7	0.3	
n-heptane[e]	3.4831	3.8049	238.40	2.0	0.3	
n-octane[e]	3.8176	3.8373	242.78	1.6	0.8	
cyclohexane[e]	2.5303	3.8499	278.11	3.1	0.5	
cycloheptane[d,f]	2.6956	3.9403	296.05	0.5	0.3	
1-pentanol[g]	3.6260	3.4508	247.28	0.5	0.5	
water[h]	1.5000	2.6273	180.30	2.6	0.9	

[a] See text for details on adopted molecular models. [b] See eq 7. [c] Reference 17. [d] This work. [e] Reference 36. [f] Parameters were regressed by use of the data set of 20 equidistant points for vapor pressure and saturated liquid at 0.5−0.9 reduced temperature data taken from the DIPPR data compilation of ref 74. [g] Two-site (2B) model: ε^{AB}/k_B = 2252.1 K; κ^{AB} = 0.010 319. Taken from ref 37 [h] Four-site (4C) model: ε^{AB}/k_B = 1804.22 K; κ^{AB} = 0.0942. Taken from ref 75

UNIFAC are required for k_{ij} calculations. The number of predicted γ_i^{∞} data points, as well as the range of temperature for k_{ij} parameter fitting, depends on the type of thermodynamic data taken into consideration. For example, to predict binary LLE phase diagram in a given temperature range, a few γ_i^{∞} predicted values in this temperature range and an appropriate relationship between k_{ij} and temperature (e.g., linearity) are required. In turn, for isothermal binary VLE data, a single γ_i^{∞} predicted value at the temperature of VLE conditions is necessary.

Of course, the proposed methodology can be applied only if it is possible to represent the molecular structure of the IL as the sum of building blocks defined by the group-contribution model. Unfortunately, the current version of model UNIFAC (Dortmund) reported recently by Nebig and Gmehling[33] lacks the necessary functional groups for piperidinium ILs, and hence in this paper we used experimental values of γ_i^{∞} measured in our laboratory.[14,18] However, we will test the performance of the outlined method in future studies for other families of ILs with imidazolium, pyridinium, or pyrrolidinium cations and [NTf_2] anion.

RESULTS AND DISCUSSION

Experimental Results. In this section we summarize and discuss the reported experimental data of density of pure [BMPIP][NTf_2] and binary LLE for 10 investigated systems (IL + hydrocarbon).

Density. Experimental densities of [BMPIP][NTf_2] in the temperature range T = 293.15−363.15 K are listed in Table 1. The results can be described by the following linear dependence:

$$\ln \rho/\mathrm{g\cdot cm^{-1}} = 0.32147 - 6.23\cdot 10^{-4}(T/\mathrm{K} - 298.15) \tag{6}$$

with squared regression coefficient R^2 = 0.999 994. The measured data are in very good agreement with literature values.[19,26,69] As expected, density of pure [BMPIP][NTf_2] is lower in comparison with pure [PMPIP][NTf_2].[17] The increase of molar volume corresponding to addition of one CH_2 group to the side chain in cation is about 17 $cm^3\cdot mol^{-1}$. That value is exactly the

Table 4. NRHB Pure Fluid Molecular Parameters for ILs and Other Substances Investigated in This Work[a]

fluid	ε_h (J·mol^{-1})	ε_s (J·mol^{-1}·K^{-1})	$v_{sp,0}$[b] (cm^3·g^{-1})	s	% AARD[c] ρ	% AARD[c] P	% AARD[c] δ_{tot}
[PMPIP][NTf$_2$][d]	5959.3	3.41241	0.67933	0.823	<0.1		0.1
[BMPIP][NTf$_2$][e]	5908.7	4.40640	0.69401	0.822	<0.1		0.1
n-hexane[f]	3957.1	1.6580	1.27753	0.857	0.5	1.1	
n-heptane[f]	4042.0	1.7596	1.25328	0.850	0.5	0.5	
n-octane[f]	4105.3	1.8889	1.23687	0.844	0.7	0.4	
cyclohexane[f]	4469.2	1.8391	1.19596	0.801	0.6	0.9	
cycloheptane[e,g]	4613.7	2.0979	1.16695	0.801	1.8	0.8	
1-pentanol[h]	4471.7	1.55212	1.12869	0.857	1.4	0.4	
water[i]	5336.5	−6.5057	0.97034	0.861	2.0	1.3	

[a] See text for details on adopted molecular models. [b] $v_{sp,1}$ is set to 0.150×10^{-3} cm^3·g^{-1}·K^{-1} for ILs, -0.412×10^{-3} cm^3·g^{-1}·K^{-1} for hydrocarbons, -0.310×10^{-3} cm^3·g^{-1}·K^{-1} for 1-pentanol, and -0.300×10^{-3} cm^3·g^{-1}·K^{-1} for water.[42] [c] See eq 7. [d] Reference 17. [e] This work. [f] Reference 75. [g] Parameters were regressed by use of the data set of 20 equidistant points for vapor pressure and saturated liquid at 0.5−0.9 reduced temperature data taken from the DIPPR data compilation of ref 74. [h] Two-site (2B) model: $E_{\alpha\beta}^{H} = -24\,000$ J·mol^{-1}, $S_{\alpha\beta}^{H} = -27.5$ J·mol^{-1}·K^{-1}. Taken from ref 50 [i] Four-site (4C) model: $E_{\alpha\beta}^{H} = -16\,100$ J·mol^{-1}, $S_{\alpha\beta}^{H} = -14.7$ J·mol^{-1}·K^{-1}. Taken from ref 50

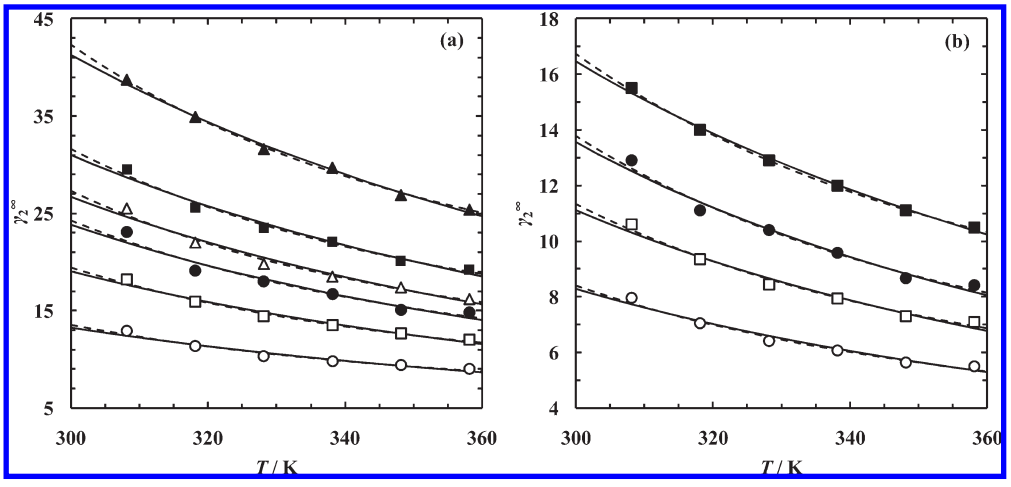

Figure 3. Limiting activity coefficients γ_2^∞ of hydrocarbons in investigated Iionic liquids. (a) *n*-Alkanes in [PMPIP][NTf$_2$] (●, *n*-hexane; ■, *n*-heptane; ▲, *n*-octane) and in [BMPIP][NTf$_2$] (○, *n*-hexane; □, *n*-heptane; Δ, *n*-octane). (b) Cycloalkanes in [PMPIP][NTf$_2$] (●, cyclohexane; ■, cycloheptane) and in [BMPIP][NTf$_2$] (○, cyclohexane; □, cycloheptane). (—) PC-SAFT model; (---) NRHB model.

same as that obtained for [NTf$_2$]-based ILs with imidazolium cations.[70] Moreover, the value 6.23×10^{-4} K^{-1} of the isobaric expansion coefficient is almost exactly the same as in the case of the IL [PMPIP][NTf$_2$].[17]

Binary Liquid−Liquid Equilibrium. For the present study, liquid-phase behavior for 10 binary (IL + *n*-alkane or cycloalkane) systems was determined for IL-rich mixtures. The resulting mole fractions of IL and corresponding LLE temperatures are given in Table 2. The results are quite typical for systems with ILs. For all systems, the increase of solubility with increasing temperature is observed. Therefore the LLE diagrams have shapes typical for diagrams with upper critical solution temperature. For the same IL, the miscibility gap increases with increasing length of the *n*-alkane chain. Solubility of cyclohexane and cycloheptane in ILs is better than that of corresponding alkanes *n*-hexane and *n*-heptane. Such behavior confirms the well-known rule *similia similibus solvuntur*, suggesting that aliphatic hydrocarbons with cyclic structure, analogous to 1-alkyl-1-methylpiperidinium cation structure, should be more soluble in IL than *n*-alkanes. Moreover, solubility of *n*-alkane or cycloalkane in the IL increases with increasing length of *N*-substituted alkyl chain in the cation. The same trends were observed for systems with other ILs.[71−73] Moreover, solubilities of all hydrocarbons in [BMPIP][NTf$_2$] are higher than in the hydrophilic IL [BMPIP][SCN].[16]

Modeling. In the following section we present and discuss results of modeling of pure ILs and calculations of binary interaction parameters and binary LLE in studied systems (IL + hydrocarbon).

Pure Fluids. In the beginning, the molecular parameters for [PMPIP][NTf$_2$] were taken from our previous work.[17] Those parameters, calculated only on the basis of atmospheric pressure data, were tested by comparing predicted densities at high pressure with experimental data of Gardas et al.[29] Resulting average absolute relative deviation (% AARD) of density at temperature $T = 293.15-393.15$ K and pressure $P = 0.1-35$ MPa is 0.31 and 0.26 for PC-SAFT and NRHB models (see Figure 2). Although relative error increases with increasing pressure, its value is still low and the results are in a very good agreement between

dx.doi.org/10.1021/jp205048b |J. Phys. Chem. B 2011, 115, 12537–12548

Table 5. PC-SAFT and NRHB Parameters[a] for Binary Systems

	PC-SAFT				NRHB			
	k_{12}[b]		% AARD[c]		k_{12}[b]		% AARD[c]	
solute	a_{12}	$10^5 b_{12}$	γ_2^∞	x_1	a_{12}	$10^5 b_{12}$	γ_2^∞	x_1
[PMPIP][NTf_2]								
n-hexane	0.0370	−7.99	2.80	2.45	0.0456	9.10	2.44	2.28
n-heptane	0.0323	−5.08	1.75	2.48	0.0418	12.4	1.41	2.28
n-octane	0.0302	−3.06	0.96	1.54	0.0394	14.6	0.55	1.43
cyclohexane	0.0394	−10.2	1.84	5.29	0.0565	9.76	1.59	4.46
cycloheptane	0.0366	−5.14	0.74	4.80	0.0507	14.5	0.36	4.07
1-pentanol	0.0384	−16.4	0.36	51.5[d]	0.0383	−25.2	0.40	44.2[d]
water	0.1770	−38.1	1.60	3.00	0.2133	−281	1.73	13.5
[BMPIP][NTf_2]								
n-hexane	0.0206	−7.80	2.31	3.78	0.0331	5.36	1.83	2.98
n-heptane	0.0211	−8.70	1.89	3.68	0.0336	5.41	1.34	3.13
n-octane	0.0217	−7.64	2.11	2.10	0.0334	6.86	1.49	1.87
cyclohexane	0.0248	−11.2	2.00	8.29	0.0451	5.55	1.59	6.02
cycloheptane	0.0270	−10.3	1.91	7.00	0.0439	6.97	1.43	5.30

[a] Binary interaction parameters k_{12}, temperature dependence coefficients, and average absolute relative deviations (% AARD) of limiting activity coefficients in ILs (γ_2^∞) and LLE IL mole fraction (x_1) are listed. [b] See eq 9. [c] See eq 7. [d] % AARD of IL mole fraction in IL-rich phase (% AARD of 1-pentanol mole fraction in alcohol-rich phase is 1.70 and 1.90 for PC-SAFT and NRHB models, respectively).

experiment and prediction. Therefore the set of parameters for [PMPIP][NTf_2] was not updated. The % AARD is defined as

$$\%\text{AARD} = \frac{100}{N_X}\sum_i \left|\frac{X_i^{\text{calcd}} - X_i^{\text{exptl}}}{X_i^{\text{exptl}}}\right| \tag{7}$$

where X is considered quantity (in this case density ρ) and N_X stands for number of experimental points. In this case $X = \rho$ and $N_X = 91$, including data of Paduszyński et al.[17] and Gardas et al.[29]

Pure fluid molecular parameters for [BMPIP][NTf_2] were obtained by fitting the predictions from PC-SAFT and NRHB to experimental density data reported in this paper and literature total solubility parameters determined from retention data of gas−liquid chromatography.[51] Additionally, we performed PC-SAFT and NRHB parametrizations for cycloheptane based on literature saturated liquid density and vapor pressure in the range of 0.5−0.9 reduced temperature.[74] The parameters for other hydrocarbons were taken from literature.[36,75] The calculations are summarized in Tables 3 and 4. In the following text we present arguments showing that optimized parameters are physically reliable and reflect basic features related to structure and interactions of studied ILs. Such well-behaved pure-component parameters are of great importance in many applications, because they allow us to correlate and, on demand, interpolate or extrapolate pure-component parameters to weakly characterized components.

As we expected, the values of optimized PC-SAFT parameters (m, σ, and ε/k_B) are similar but slightly higher than the corresponding values for [PMPIP][NTf_2]. In particular, the hard-sphere molar volume of [BMPIP][NTf_2], defined as $V_{hs} = N_{Av}\pi m\sigma^3/6$ where N_{Av} is Avogadro's number, should be higher than V_{hs} of [PMPIP][NTf_2]. Indeed, it is higher by about 8.5 $cm^3\cdot mol^{-1}$. This volume increment is fairly similar to that for alkanes (about 7.7 $cm^3\cdot mol^{-1}$ between *n*-heptane and *n*-hexane and about 7.5 between *n*-octane and *n*-heptane). Dispersive energy per molecule, $m\varepsilon/k_B$, is also higher for [BMPIP][NTf_2] in comparison with [PMPIP][NTf_2].

In the case of NRHB theory, only ε^*_h, ε^*_s, and $v^*_{sp,0}$ pure fluid parameters for [BMPIP][NTf_2] were obtained from optimization. Hard-core molar volume of [BMPIP][NTf_2], defined this time as $V^* = Mv^*_{sp}$ where M denotes molecular mass, equals 302.9 $cm^3\cdot mol^{-1}$, while for [PMPIP][NTf_2] it is 287.0 $cm^3\cdot mol^{-1}$ (at $T = 298.15$ K). The difference between those values (15.9 $cm^3\cdot mol^{-1}$) is almost the same as the difference between hard-core molar volumes of *n*-heptane and *n*-hexane (18.0 $cm^3\cdot mol^{-1}$) or *n*-octane and *n*-heptane (15.6 $cm^3\cdot mol^{-1}$). Dispersive energy per segment of [BMPIP][NTf_2] is lower than those for [PMPIP][NTf_2]. However, the molar dispersive energies (defined as $E^* = M\varepsilon^* v^*_{sp,0}/v^*$, where $v^* = 9.75$ $cm^3\cdot mol^{-1}$ is a segmental volume[42]) for ILs are 175.4 and 183.6 $kJ\cdot mol^{-1}$ (at $T = 298.15$ K) for [PMPIP][NTf_2] and [BMPIP][NTf_2], respectively. The difference for ILs is 8.2 $kJ\cdot mol^{-1}$, while for heptane/hexane and octane/heptane pairs the differences are respectively 8.4 and 7.4 $kJ\cdot mol^{-1}$. As mentioned in the previous section, $v^*_{sp,1}$ is treated as a characteristic parameter for different homologous series. For ILs and hydrocarbons it was set to 0.150×10^{-3} and -0.412×10^{-3} $cm^3\cdot g^{-1}$, respectively, as suggested in the original NRHB papers.[42] Finally, the parameter $s = q/r$ was estimated from the correlation we used in our previous works:[76]

$$\begin{aligned} r &= 0.029\,281 V/\text{cm}^3\cdot\text{mol}^{-1} \\ zq &= (z-2)r + 2 \end{aligned} \tag{8}$$

where V stands for liquid molar volume (cubic centimeters per mole) at $T = 298.15$ K and the lattice coordination number z is set equal to 10. The resulting value $s = 0.822$ is similar for [PMPIP][NTf_2] or imidazolium ILs with [NTf_2] anion. For cycloheptane we used the van der Waals reduced volume and van der Waals area taken from the DIPPR data compilation.[74]

Following our previous work, we assumed the presence of five positive and five negative associating sites per IL ion pair. As mentioned earlier, we used an A_1 site to represent a positive group corresponding to the positive charge of the cation and its proximity and a B_1 site to represent a negative site corresponding to the delocalized charge on the anion. Each type of associating site is identically defined, but only AB interactions between different IL molecules are allowed. In order to decrease the number of degrees of freedom of the system for fitting, the association parameters, ε^{AB} and κ^{AB} for PC-SAFT and $E_{\alpha\beta}{}^H$ and $S_{\alpha\beta}{}^H$ for NRHB, were set to be the same as those for [PMPIP][NTf_2]:[17] $\varepsilon^{AB} = 1912.1$ K, $\kappa^{AB} = 0.057\,34$, $E_{\alpha\beta}{}^H = -16\,900$ $J\cdot mol^{-1}$, and $S_{\alpha\beta}{}^H = -42.2$ $J\cdot mol^{-1}\cdot K^{-1}$. In further investigations we will keep them constant for the whole family of [NTf_2]-based piperidinium ILs, with the assumption that the alkyl chain length of the cation does not affect the strength of the associating bonds. The validity of this assumption was very recently confirmed for the imidazolium family of ILs with [NTf_2] anion.[47]

It is worth mentioning that we tested the performance of other different models as a function of number of associating groups per molecule and concluded that a five-sites model gives desired results. Models with less associating sites cause difficulties related to correlation of pure fluid properties (problems with capturing high values of solubility parameters).

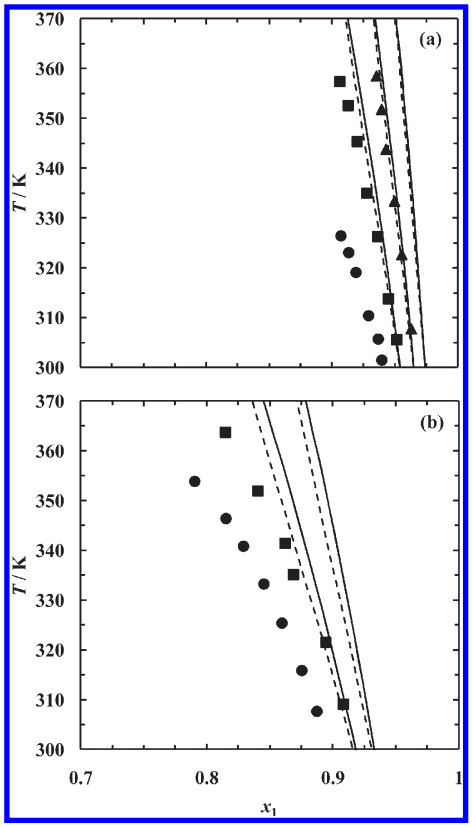

Figure 4. Experimental and calculated LLE phase diagrams (IL mole fraction x_1 vs LLE temperature T) for binary systems of [PMPIP][NTf_2] + hydrocarbon: (a) *n*-alkanes (●, *n*-hexane; ■, *n*-heptane; ▲, *n*-octane); (b) cycloalkanes (●, cyclohexane; ■, cycloheptane). (—) PC-SAFT model; (---) NRHB model.

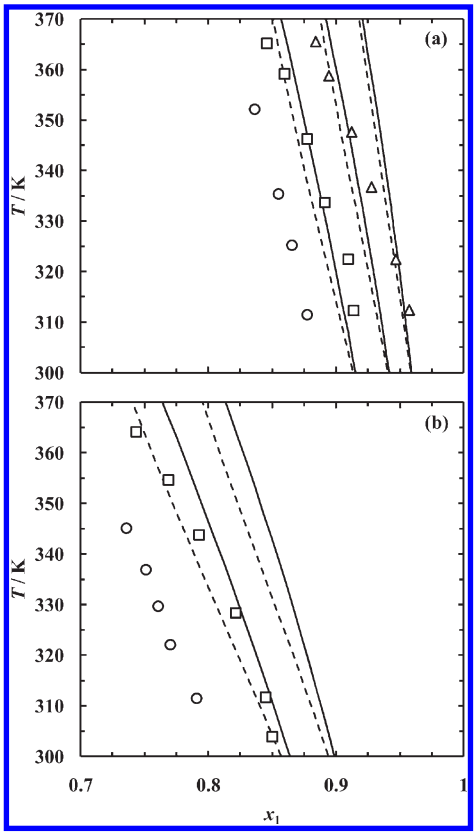

Figure 5. Experimental and calculated LLE phase diagrams (IL mole fraction x_1 vs LLE temperature T) for binary systems of [BMPIP]-[NTf_2] + hydrocarbon: (a) *n*-alkanes (○, *n*-hexane; □, *n*-heptane; Δ, *n*-octane); (b) cycloalkanes (○, cyclohexane; □, cycloheptane). (—) PC-SAFT model; (---) NRHB model.

Results of the calculations of temperature dependence of liquid density and total solubility parameter are presented in Figure 2. One can see PC-SAFT and NRHB theories are both capable of describing both properties by use of one set of parameters. The % AARD values are around 0.10 in both cases. The results of high-pressure density predictions of [PMPIP][NTf_2] are shown in Figure 2 as well.

To perform all the optimizations as well as PC-SAFT and NRHB calculations, we used MATLAB (version R2009a, Mathworks, Inc.) scripts and functions designed and coded in our laboratory.

Binary Interaction Parameter. In further text we will denote the IL ([PMPIP][NTf_2] or [BMPIP][NTf_2]) and hydrocarbon (*n*-hexane, *n*-heptane, *n*-octane, cyclohexane, or cycloheptane) by $i = 1$ and $j = 2$, respectively. Binary interaction parameters k_{12} appearing in Lorentz−Berthelot mixing rules (see eqs 3 and 4) to correct cross-interaction parameters were adjusted to literature limiting activity coefficient data of hydrocarbons in ILs, γ_2^{∞}. In order to increase the calculations' accuracy over a broader temperature range, k_{12} is allowed to be a linear function of temperature:

$$k_{12} = a_{12} + b_{12}(T/\mathrm{K} - 298.15) \qquad (9)$$

Coefficients a_{12} and b_{12} were obtained for each system by optimization sum of squares of relative deviations between calculated and experimental values of γ_2^{∞}. Limiting activity coefficients were calculated according to the formula given in eq 5.

Results of γ_2^{∞} correlation are shown in Figure 3. Values of the coefficients a_{12} and b_{12} are given in Table 5 together with average deviations defined in the same manner as in eq 7 (substituting $X = \gamma_2^{\infty}$). We see that PC-SAFT and NRHB models are capable of accurate description of the experimental data. Mean % AARD values of γ_2^{∞} for PC-SAFT and NRHB are 1.8 and 1.4. We assigned an individual set of coefficients to each IL + hydrocarbon system. However, obtained values of coefficients a_{12} are very similar for systems containing the same IL, suggesting that some universal value describing all the data could be introduced. We will consider such a method of calculations in our future studies.

Binary Liquid−Liquid Equilibrium. First, we have attempted to predict γ_2^{∞} values and LLE phase diagrams by setting $k_{12} = 0$. The results (not shown in this paper) were not satisfactory. Therefore, the pure component parameters from Tables 3 and 4, together with binary interaction parameters from Table 5, were used for the calculations of LLE in the 10 binary systems (IL + hydrocarbon). Resulting phase diagrams are shown in Figures 4 and 5. In Table 5 the % AARD of the IL mole fraction is presented. The mean values of % AARD are 4.1 and 3.4 for PC-SAFT and NRHB models, respectively, while deviations of calculations from experiment become larger for higher temperatured. According to the models' predictions, solubility of hydrocarbons in ILs is lower than evidenced by measurements. Then, it can be concluded that PC-SAFT and NRHB models are able to capture phase behavior in a qualitative manner. Both models predict the

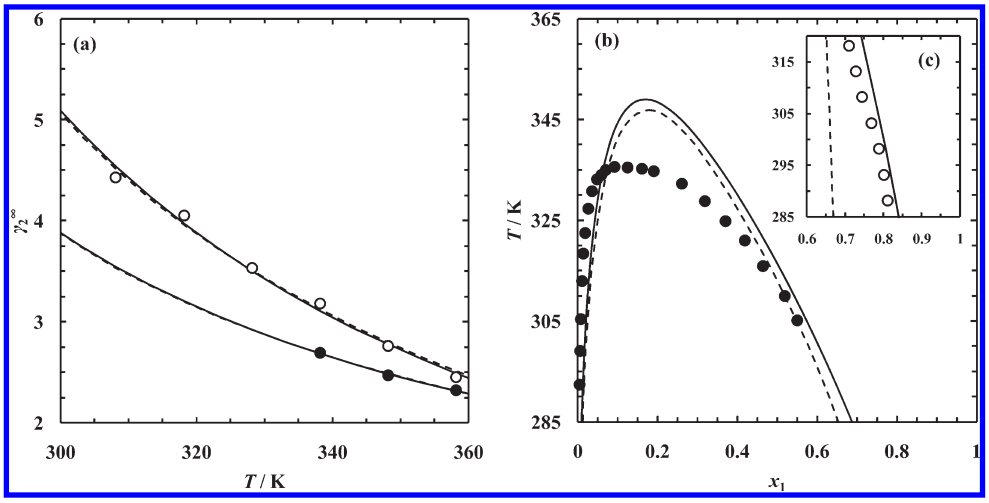

Figure 6. PC-SAFT and NRHB calculations for cross-associating IL-systems: (a) limiting activity coefficients of 1-pentanol (●) and water (○) in [PMPIP][NTf_2];[14] (b) LLE in binary system [PMPIP][NTf_2] + 1-pentanol;[17] (c) LLE in binary system [PMPIP][NTf_2] + water.[28] (—) PC-SAFT model; (---) NRHB model.

order in which solubility of hydrocarbon in IL increases, including the effects of chain length of *n*-alkane as well as chain length of alkyl substituent in piperidinium cation. Moreover, the predicted solubility of cycloalkanes is also higher than that of respective *n*-alkanes.

We decided to check how the applied approach works for cross-associating systems [PMPIP][NTf_2] + alcohol, presented by us previously, and for [PMPIP][NTf_2] + water, reported by Freire et al.[27,28] Unfortunately γ_2^∞ data are available only for short-chain alcohols (from methanol to 1-pentanol) and for water.[14] Thus, we performed calculations only for systems with 1-pentanol and water. The models' parameters for pure 1-pentanol and water were taken from literature.[50,75] They are summarized in Tables 3 and 4. For 1-pentanol, a two-site association scheme (2B) was assumed for both models, while in the case of water, four-site (4C) models were adopted in both PC-SAFT and NRHB theories. Standard mixing rules were used to obtain cross-association parameters corresponding to interactions between associating sites A_1 and B_1 of the IL and A_2 and B_2 of 1-pentanol or water:

$$\varepsilon^{A_1B_2} = \frac{\varepsilon^{A_1B_1} + \varepsilon^{A_2B_2}}{2} \qquad \kappa^{A_1B_2} = \sqrt{\kappa^{A_1B_1}\kappa^{A_2B_2}}\left(\frac{2\sqrt{\sigma_1\sigma_2}}{\sigma_1 + \sigma_2}\right)^3$$

$$E^{H}_{A_1B_2} = \frac{E^{H}_{A_1B_1} + E^{H}_{A_2B_2}}{2} \qquad S^{H}_{A_1B_2} = \left[\frac{(S^{H}_{A_1B_1})^{1/3} + (S^{H}_{A_2B_2})^{1/3}}{2}\right]^3 \tag{10}$$

Interactions A_1A_2 and B_1B_2 were not allowed. Finally, it should be emphasized that literature PC-SAFT parameters for water used in the present calculations were originally optimized for a simplified version of PC-SAFT proposed by von Solms et al. (sPC-SAFT).[77] However, we checked that those parameters can be used with original PC-SAFT to accurately reproduce vapor pressures and densities in the range of 0.5−0.9 reduced temperature.

The summary of calculations is showed in Figure 6, while optimized values of binary interaction parameters and % AARD of γ_2^∞ and IL mole fraction are collected in Table 5. It can be noticed that γ_2^∞ of 1-pentanol and water are described by PC-SAFT and NRHB with practically the same accuracy. In the case of the [PMPIP][NTf_2] + water system, the values of binary interaction parameters are higher than corresponding values for the [PMPIP][NTf_2] + 1-pentanol system. Moreover, the values of coefficients a_{12} and b_{12} are similar in the case of both models applied.

Results of LLE calculations are also promising. Binary system [PMPIP][NTf_2] + 1-pentanol is well described by both models, but differences between experimental and predicted LLE compositions become larger as the temperature increases. On the other hand, the asymmetric shape of the LLE curve is well captured by PC-SAFT and NRHB, but the upper critical solution temperature is still overestimated by about 15 K. In the case of the system [PMPIP][NTf_2] + water, PC-SAFT gives surprisingly excellent results if we take into account the IL-rich phase. Experimental solubility of the IL in water (water-rich phase),[27] however, is much higher than the predicted values by several orders of magnitude (not shown in Figure 6). In our opinion, it might be due to the molecular model of the IL, which is not suitable for dilute solutions of ILs in water. One can suspect that, in the range of very low concentration of IL in such a polar solvent as water, cations and anions occur as individual moieties and solvation becomes an essential factor, increasing the solubility.

CONCLUDING REMARKS

We reported new experimental results on liquid density of [BMPIP][NTf_2] and LLE measurements of binary systems composed of [PMPIP][NTf_2] or [BMPIP][NTf_2] ILs and hydrocarbon (*n*-hexane, *n*-heptane, *n*-octane, cyclohexane, or cycloheptane). As expected, molar volume of [BMPIP][NTf_2] is higher than of [PMPIP][NTf_2] by about 17 $cm^3 \cdot mol^{-1}$. Typical results of LLE, observed for system with different ILs, were obtained, including (1) upper critical solution temperature phase behavior for all studied systems, (2) decrease of solubility of hydrocarbon with increasing alkyl chain length, and (3) increase of solubility upon changing from linear into cyclic structure of hydrocarbon.

Modeling of LLE of investigated systems was performed in terms of two modern theories, PC-SAFT and NRHB. Pure fluid parameters of the models were obtained from fitting of

experimental liquid density and solubility parameter data in the temperature range T = 293.15−363.15 K at ambient pressure. Both models are able to describe these two quantities within the mean % AARD = 0.1. Quality of obtained parameters was tested against high-pressure density data of [PMPIP][NTf_2], which were not employed in the optimization procedure. Resulting deviations on the order of 0.2 prove the reliability of the parameters.

Both models used in a purely predictive manner (i.e., without introduction of binary parameters) did not give good results. Therefore, reported previously activity coefficients of *n*-alkanes and cycloalkanes at infinitely diluted mixtures with ILs were used to optimize binary interaction parameters k_{12} involved in standard Lorentz−Berthelot mixing rules. By use of obtained values of k_{12}, binary LLE phase diagrams were calculated, resulting in average absolute relative deviations (% AARD) for the IL mole fraction of 4.1 and 3.4 for PC-SAFT and NRHB, respectively. To test the performance of the applied procedure of calculations, we additionally calculated LLE phase diagrams for binary systems of [PMPIP][NTf_2] with associating component (1-pentanol and water). Obtained results are relatively good in spite of the simplicity of adopted molecular models and combining rules for cross-association parameters.

In summary, this study provides another set of experimental data on binary systems with ILs. Moreover, we hope that modeling presented in this paper may give some insight into performance of molecular-based thermodynamic models of such systems.

AUTHOR INFORMATION

Corresponding Author

*E-mail kpaduszynski@ch.pw.edu.pl.; phone +48 22 234 5640.

ACKNOWLEDGMENT

This work has been supported by the European Union in the framework of European Social Fund through the Warsaw University of Technology Development Programme.

REFERENCES

(1) Plechkova, N. V.; Seddon, K. R. *Chem. Soc. Rev.* **2008**, *37*, 123–150.
(2) Roosen, C.; Müller, P.; Greiner, L. *Appl. Microbiol. Biotechnol.* **2008**, *81*, 607.
(3) Moniruzzaman, M.; Kamiya, N.; Goto, M. *J. Colloid Interface Sci.* **2010**, *352*, 136–142.
(4) Bogel-Łukasik, E.; Santos, S.; Bogel-Łukasik, R.; Nunes da Ponte, M. *J. Supercrit. Fluids* **2010**, *54*, 210–217.
(5) Opperman, S.; Stein, F.; Kragl, U. *Appl. Microbiol. Biotechnol.* **2011**, *89*, 439–499.
(6) Armand, M.; Endres, F.; MacFarlane, D. R.; Ohno, H.; Scrosati, B. *Nat. Mater.* **2009**, *8*, 621–629.
(7) Cao, Y.; Zhang, J.; Bai, Y.; Renzhi, L.; Zakeeruddin, S. M.; Grätzel, M.; Wang, P. *J. Phys. Chem. C* **2008**, *112*, 13775–13781.
(8) Yu, G.; Li, X.; Asumana, C.; Chen, X. *Ind. Eng. Chem. Res.* **2011**, *50*, 2236–2244.
(9) Kedra-Królik, K.; Mutelet, F.; Jaubert, J.-N. *Ind. Eng. Chem. Res.* **2011**, *50*, 2296–2306.
(10) Varma, N. R.; Ramalingam, A.; Banerjee, T. *Chem. Eng. J.* **2011**, *166*, 30–39.
(11) Shiflett, M. B.; Shiflett, A. D.; Yokozeki, A. *Sep. Purif. Technol.* **2011**, *79*, 357–364.
(12) Myers, C.; Pennline, H.; Luebke, D.; Ilconich, J.; Dixon, J. K.; Maginn, E. J.; Brennecke, J. F. *J. Membr. Sci.* **2008**, *322*, 28–31.
(13) Muldoon, M. J.; Aki, S. N. V. K.; Anderson, J. L.; Dixon, J. K.; Brennecke, J. F. *J. Phys. Chem. B* **2007**, *111*, 9001–9009.
(14) Domańska, U.; Paduszyński, K. *J. Chem. Thermodyn.* **2010**, *42*, 1361–1366.
(15) Domańska, U.; Królikowska, M. *J. Chem. Eng. Data* **2011**, *56*, 124–129.
(16) Domańska, U.; Królikowska, M.; Paduszyński, K. *Fluid Phase Equilib.* **2011**, *303*, 1–9.
(17) Paduszyński, K.; Chiyen, J.; Ramjugernath, D.; Letcher, T. M.; Domańska, U. *Fluid Phase Equilib.* **2011**, *305*, 45–52.
(18) Paduszyński, K.; Domańska, U. *J. Phys. Chem. B* **2011**, *115*, 8207–8215.
(19) Bazito, F. F. C.; Kawano, Y.; Torresi, R. M. *Electrochim. Acta* **2007**, *52*, 6427–6437.
(20) Mun, J.; Jung, Y. S.; Yim, T.; Lee, H. Y.; Kim, H.-J.; Kim, Y. G.; Oh, S. M. *J. Power Sources* **2009**, *194*, 1068–1074.
(21) Rodopoulos, T.; Smith, L.; Horne, M. D.; Rüther, T. *Chem.—Eur. J.* **2010**, *16*, 3815–3826.
(22) Liu, K.; Zhou, Y.-X.; Han, H.-B.; Zhou, S.-S.; Feng, W.-F.; Nie, J.; Li, H.; Huang, X.-J.; Armand, M.; Zhou, Z.-B. *Electrochim. Acta* **2010**, *55*, 7145–7151.
(23) Fang, S.; Zhang, Z.; Jin, Y.; Yang, L.; Hirano, S.-I.; Tachibana, K.; Katayama, S. *J. Power Sources* **2011**, *196*, 5637–5644.
(24) Tsuda, T.; Kondo, K.; Tomioka, T.; Takahashi, Y.; Matsumoto, H.; Kuwubata, S.; Hussey, C. L. *Angew. Chem., Int. Ed.* **2011**, *50*, 1310–1313.
(25) Sun, X.-G.; Dai, S. *Electrochim. Acta* **2010**, *55*, 4618–4626.
(26) Montanino, M.; Carewska, M.; Alessandrini, F.; Passerini, S.; Appetecchi, G. B. *Electrochim. Acta* **2011**, DOI:10.1016/j.electacta.2011.03.089.
(27) Freire, M. G.; Neves, C. M. S. S.; Ventura, S. P. M.; Pratas, M. J.; Marrucho, I. M.; Oliviera, J.; Coutinho, J. A. P.; Fernandes, A. M. *Fluid Phase Equilib.* **2010**, *294*, 234–240.
(28) Freire, M. G.; Neves, C. M. S. S.; Carvalho, P. J.; Gardas, R. L.; Fernandes, A. M.; Marrucho, I. M.; Santos, L. M. N. B. F.; Coutinho, J. A. P. *J. Phys. Chem. B* **2007**, *111*, 13082–13089.
(29) Gardas, R. L.; Costa, H. F.; Freire, M. G.; Carvalho, P. J.; Marrucho, I. M.; Fonseca, I. M. A.; Ferreira, A. G. M.; Coutinho, J. A. P. *J. Chem. Eng. Data* **2008**, *53*, 805–811.
(30) Vega, L. F.; Vilaseca, O.; Llovell, F.; Andreu, J. S. *Fluid Phase Equilib.* **2010**, *294*, 15–30.
(31) Domańska, U.; Królikowski, M.; Paduszyński, K. *J. Chem. Thermodyn.* **2009**, *41*, 932–938.
(32) Yokozeki, A.; Shiflett, M. B. *J. Supercrit. Fluids* **2010**, *55*, 846–851.
(33) Nebig, S.; Gmehling, J. *Fluid Phase Equilib.* **2011**, *302*, 220–225.
(34) Chapman, W. G.; Gubbins, K. E.; Jackson, G.; Radosz, M. *Fluid Phase Equilib.* **1989**, *52*, 31–38.
(35) Chapman, W. G.; Gubbins, K. E.; Jackson, G.; Radosz, M. *Ind. Eng. Chem. Res.* **1990**, *29*, 1709–1721.
(36) Gross, J.; Sadowski, G. *Ind. Eng. Chem. Res.* **2001**, *40*, 1244–1260.
(37) Gross, J.; Sadowski, G. *Ind. Eng. Chem. Res.* **2002**, *41*, 5510–5515.
(38) Blas, F. J.; Vega, L. F. *Mol. Phys.* **1997**, *92*, 135–150.
(39) Karakatsani, E. K.; Economou, I. G. *J. Phys. Chem. B* **2006**, *110*, 9252–9261.
(40) Karakatsani, E. K.; Kontogeorgis, G. M.; Economou, I. G. *Ind. Eng. Chem. Res.* **2006**, *45*, 6063–6074.
(41) Panayiotou, C.; Pantoula, M.; Stefanis, E.; Tsivintzelis, I.; Economou, I. G. *Ind. Eng. Chem. Res.* **2004**, *43*, 6592–6606.
(42) Panayiotou, C.; Tsivintzelis, I.; Economou, I. . *Ind. Eng. Chem. Res.* **2007**, *46*, 2628–2636.
(43) Xu, X.; Peng, C.; Liu, H.; Hu, Y. *Fluid Phase Equilib.* **2011**, *302*, 260–268.
(44) Currás, M. R.; Vijande, J.; Piñeiro, M. M.; Lugo, L.; Salgado, J.; García, J. *Ind. Eng. Chem. Res.* **2011**, *50*, 4065–4076.

(45) Andreu, J. S.; Vega, L. F. *J. Phys. Chem. C* **2007**, *111*, 16028–16034.
(46) Andreu, J. S.; Vega, L. F. *J. Phys. Chem. B* **2008**, *112*, 15398–15406.
(47) Llovell, F.; Valente, E.; Vilaseca, O.; Vega, L. F. *J. Phys. Chem. B* **2011**, *115*, 4387–4398.
(48) Kroon, M. C.; Karakatsani, E. K.; Economou, I. G.; Witkamp, G.-J.; Peters, C. J. *J. Phys. Chem. B* **2006**, *110*, 9262–9269.
(49) Karakatsani, E. K.; Economou, I. G.; Kroon, M. C.; Peters, J. C.; Witkamp, G.-J. *J. Phys. Chem. C* **2007**, *111*, 15487–15492.
(50) Tsioptsias, C.; Tsivintzelis, I.; Panayiotou, C. *Phys. Chem. Chem. Phys.* **2010**, *12*, 4843–4851.
(51) Marciniak, A. *Int. J. Mol. Sci.* **2011**, *12*, 3553–3575.
(52) Schacht, C. S.; Zubeir, L.; de Loos, T. W.; Gross, J. *Ind. Eng. Chem. Res.* **2010**, *49*, 7646–7653.
(53) Domańska, U. *Fluid Phase Equilib.* **1986**, *26*, 201–220.
(54) Wertheim, M. S. *J. Stat. Phys.* **1984**, *35*, 35–47.
(55) Wertheim, M. S. *J. Stat. Phys.* **1986**, *42*, 477–492.
(56) Müller, E. A.; Gubbins, K. E. *Ind. Eng. Chem. Res.* **2001**, *40*, 2193–2211.
(57) Economou, I. G. *Ind. Eng. Chem. Res.* **2002**, *41*, 953–962.
(58) Tan, S. P.; Adirama, H.; Radosz, M. *Ind. Eng. Chem. Res.* **2008**, *47*, 8063–8082.
(59) Gross, J.; Vrabec, J. *AIChE J.* **2006**, *52*, 1194–1204.
(60) Jog, P.; Chapman, W. G. *Mol. Phys.* **1999**, *97*, 307–319.
(61) Karakatsani, E. K.; Spyriouni, T.; Economou, I. G. *AIChE J.* **2005**, *51*, 2328–2342.
(62) Shimizu, K.; Tariq, M.; Costa Gomes, M. F.; Rebelo, L. P. N.; Canongia Lopes, J. N. A. *J. Phys. Chem. B* **2010**, *114*, 5831–5834.
(63) Tsuzuki, S.; Tokuda, H.; Hayamizu, K.; Watanabe, M. *J. Phys. Chem. B* **2005**, *109*, 16474–16481.
(64) Katoh, R.; Hara, M.; Tsuzuki, S. *J. Phys. Chem. B* **2008**, *112*, 15426–15430.
(65) Fernandes, A. M.; Rocha, M. A. A.; Freire, M. G.; Marrucho, I. M.; Coutinho, J. A. P.; Santos, L. M. N. B. F. *J. Phys. Chem. B* **2011**, *115*, 4033–4041.
(66) Weiss, V. C.; Heggen, B.; Müller-Plathe, F. *J. Phys. Chem. C* **2010**, *114*, 3599–3608.
(67) Canongia Lopes, J. N. A.; Padua, A. A. H. *J. Phys. Chem. B* **2006**, *110*, 3330–3335.
(68) Triolo, A.; Russina, O.; Fazio, B.; Appetecchi, G. B.; Carewska, M.; Passerini, S. *J. Chem. Phys.* **2009**, *130*, 164521.
(69) Zhou, Z.-B.; Matsumoto, H.; Tatsumi, K. *Chem.—Eur. J.* **2006**, *12*, 2196–2212.
(70) Tariq, M.; Serro, A. P.; Mata, J. L.; Saramago, B.; Esperança, J. M. S. S.; Canongia Lopes, J. N.; Rebelo, L. P. N. *Fluid Phase Equilib.* **2010**, *294*, 131–138.
(71) Marciniak, A.; Karczemna, E. *Fluid Phase Equilib.* **2011**, *304*, 121–124.
(72) Marciniak, A. *J. Chem. Eng. Data* **2011**, *56*, 368–374.
(73) Marciniak, A.; Karczemna, E. *J. Phys. Chem. B* **2010**, *114*, 5470–5474.
(74) Design Institute for Physical Properties, Sponsored by AIChE [2005; 2008; 2009; 2010]. DIPPR Project 801, Full Version. Design Institute for Physical Property Research/AIChE. Online version available at http://knovel.com/web/portal/browse/display?_EXT_KNOVEL_DISPLAY_bookid=1187&VerticalID=0.
(75) Tsivintzelis, I.; Grenner, A.; Economou, I. G.; Kontogeorgis, G. M. *Ind. Eng. Chem. Res.* **2008**, *47*, 5651–5659.
(76) Hofman, T.; Nagata, I. *Fluid Phase Equilib.* **1986**, *25*, 113–128.
(77) von Solms, N.; Michelsen, M. L.; Kontogeorgis, G. M. *Ind. Eng. Chem. Res.* **2003**, *42*, 1098–1105.